Available online at www.sciencedirect.com
SCIENCE DIRECT®
Deep-Sea Research I 52 (2005) 179–188
DEEP-SEA RESEARCH PART I
www.elsevier.com/locate/dsr

A note on the validity of the Sverdrup balance in the Atlantic North Equatorial Countercurrent

Ariane Verdy[a,*], Markus Jochum[b]

[a]MIT / WHOI Joint Program in Oceanography, Massachusetts Institute of Technology, Cambridge MA 02139, USA
[b]Department of Earth, Atmospheric and Planetary Sciences, Massachusetts Institute of Technology, Cambridge MA 02139, USA

Received 9 September 2003; received in revised form 10 May 2004; accepted 18 May 2004

Abstract

An ocean general circulation model of the tropical Atlantic Ocean is used to study the vertically integrated vorticity equation for the annual mean flow in the Atlantic North Equatorial Countercurrent (NECC). It is found that the nonlinear terms play an important role in the vorticity budget, in the western part of the basin. Sverdrup balance does not hold in the region of the North Brazil Current retroflection, where advection of relative vorticity by the mean flow and by the eddies is important. In the eastern part of the basin, these nonlinearities are negligible and the flow appears to be in Sverdrup balance. In the model, the cut-off location occurs at 32°W. The results suggest that in the western part of the basin, observations relying on hydrographic data neglect two important contributions to the vorticity balance: advection of planetary vorticity by the deep meridional flow and advection of relative vorticity.

Keywords: Equatorial oceanography; Tropical Atlantic; Sverdrup balance; Vorticity

1. Introduction

The Atlantic North Equatorial Countercurrent (NECC) is one of the major Atlantic currents and a core component of the climate system. Its position coincides with the location of the Atlantic's warmest waters (Enfield and Mayer, 1997) and it is a major path for the warm water return flow of the global meridional overturning circulation (Fratantoni et al., 2000; Jochum and Malanotte-Rizzoli, 2001). Therefore, understanding the NECC dynamics is a prerequisite for the analysis of global and tropical Atlantic climate.

Sverdrup (1947) explained the Pacific NECC as the result of a balance between vortex stretching induced by the wind and advection of planetary vorticity. His original paper is still one of the pillars of physical oceanography and the

*Corresponding author. Tel.: +1 617 253 9345; fax: +1 617 253 6208.
E-mail address: averdy@ocean.mit.edu (A. Verdy).

0967-0637/$ - see front matter © 2004 Elsevier Ltd. All rights reserved.
doi:10.1016/j.dsr.2004.05.014

"Sverdrup balance" is used to analyze ocean circulation almost everywhere outside the equatorial regions and the western boundary currents. Most recently, Yu et al. (2000) used the Sverdrup balance to analyze the Pacific NECC.

In spite of the successes of the Sverdrup balance, it has been difficult to demonstrate its validity experimentally (Leetmaa et al., 1981; Wunsch and Roemmich, 1985; Kessler et al., 2003). More specifically, a recent study by Jochum and Malanotte-Rizzoli (2003) shows that the Atlantic NECC is barotropically unstable, implying that the advection of relative vorticity is larger than the advection of planetary vorticity (Pedlosky, 1979). This violates the major assumption of the Sverdrup balance, that advection of relative vorticity is negligible.

The vorticity balance of the Atlantic NECC has been analyzed by Garzoli and Katz (1983) between 46°W and 10°W. From historical wind and hydrographic data they concluded that the NECC is in Sverdrup balance in the interior of the basin, from 42°W to 22°W. Outside this range the vorticity budget could not be closed. Garzoli and Katz (1983) suspected that nonlinearities and lateral diffusion might be important near the western and eastern boundaries.

The present study is a continuation of their work. Since the observational data base in the Atlantic is still not sufficient to determine the complete vorticity balance in the NECC, we used a numerical model of the tropical Atlantic ocean instead. After a brief model description in Section 2, the vorticity balance is analyzed in Section 3. Section 4 summarizes the results and discusses how the nonlinear dynamics affect the validity of the Sverdrup balance and influence our understanding of tropical ocean circulation.

2. Model description

The Princeton Ocean Model (version MOM2b) with simplified geometry is used to study the circulation in the tropical Atlantic, specifically the North Brazil Current/North Equatorial Countercurrent (NBC/NECC) retroflection region. The basin extends from 25°S to 30°N, with idealized American and African coastlines and a constant depth of 3000 m. The flat bottom is not a realistic representation of the Atlantic seafloor, especially in the region of the mid-Atlantic ridge; nevertheless, due to the strong tropical stratification, the impact of topography on surface circulation is negligible (Philander, 1990). This argument is supported by the success of reduced gravity models in modelling tropical ocean circulation (Murtugudde et al., 1996). The model was spun up for 20 years and the following 4 years are analyzed in this study. The short spin up time is justified by the fast adjustment of the tropical circulation (Liu and Philander, 1995).

In the region considered here (0–12°N), the resolution is $\frac{1}{4}^\circ$ in latitude, and in longitude it ranges from $\frac{1}{4}^\circ$ near the coast of Brazil to 1° towards the eastern part of the basin. There are 30 vertical layers with a 10 m resolution in the top 100 m. The model is forced by climatological wind stress from Hellerman and Rosenstein (1983). Salinity is kept constant at a value of 35 psu; viscosity and diffusivity vary between 200 and 2000 m^2/s, depending on the spatial resolution. The configuration of the model is described in more detail in Jochum and Malanotte-Rizzoli (2003).

Comparisons of the circulation in the model with the observed circulation in the tropical Atlantic (Jochum and Malanotte-Rizzoli, 2003; Jochum et al., 2004) suggest that, although it is idealized, the model reproduces the current strength and mesoscale variability observed in the western and central tropical Atlantic. The simulated zonal velocity at 38°W in April is shown in Fig. 1. One can see the NECC centered at 6°N, the South Equatorial Current at 3°N and the Equatorial Undercurrent (EUC) just north of the equator.

In Fig. 2, the model zonal transport at 38°W is compared with observations from Katz (1993). The transport is evaluated in the top 500 m, between 3°N and 9°N. Katz (1993) calculated the geostrophic transport, relative to the 500-db level, from estimates of dynamic height derived from inverted echo sounder measurements of acoustic travel time. For consistency the model transport is also expressed relative to the 500-db

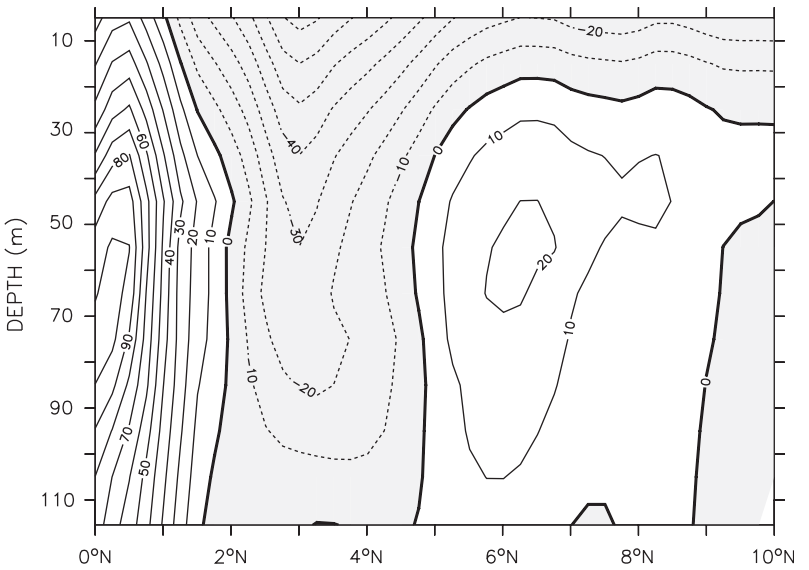

Fig. 1. The zonal velocity across 38°W in April (in cm/s). The eastward NECC can be seen at 6°N, the westward South Equatorial Current at 3°N, the EUC just north of the equator, and the westward Ekman flow everywhere in the upper 20 m.

level, although it is not significantly different when expressed relative to the bottom. The model overestimates by approximately 5 Sv, but captures the seasonal cycle of the zonal transport, with maximum transport during the fall at around 30 Sv and minimum transport during spring. The geostrophic transport is eastward throughout the year, but weakened from February to May. During that period the northeast trade winds drive a westward surface flow, which counters and overwhelms the geostrophic flow, causing the reversal of the NECC; the rest of the year, the Ekman flow is eastward and adds to the geostrophic flow (Richardson et al., 1992). This compensation between the geostrophic NECC and Ekman transports can be seen in Fig. 1.

Interestingly, the simulated transport exhibits interannual variability, in spite of the climatological wind forcing. The year to year variation in the maximum transport is approximately 5 Sv in the model and 7 Sv in the observations (Katz, 1993). This implies that a substantial part of the observed interannual variability could be explained by ocean dynamics rather than by changes in the wind field.

3. Vorticity balance

3.1. Vertically integrated vorticity equation

The vorticity equation is derived in Pedlosky (1979); here, we merely state its final form

$$\int (\overline{\vec{u}} \cdot \nabla)\overline{\zeta}\,\mathrm{d}z + \int \overline{(\vec{u}' \cdot \nabla)\zeta'}\,\mathrm{d}z + \beta\overline{V} = \frac{1}{\rho_0}\,\mathrm{curl}_z \int \vec{F}\,\mathrm{d}z + \frac{\mathrm{curl}_z\,\vec{\tau}}{\rho_0}, \quad (1)$$

where the primed quantities are the deviations from a 4-year mean. V represents meridional transport, ζ is the relative vorticity, curl_z is the vertical component of the curl operator; $\vec{\tau}$ is the surface wind stress, ρ_0 is the reference density of seawater, and $\vec{F}$ is the horizontal friction, parametrized as $A_h\nabla_h^2\overline{\vec{u}}$. The steady, linear and non-viscous approximation to Eq. (1), assuming a flat bottom and a rigid lid, yields the familiar *Sverdrup balance*, in which case the vorticity input by the wind is compensated by the meridional advection of planetary vorticity

$$\beta\overline{V} = \frac{\mathrm{curl}_z\,\vec{\tau}}{\rho_0}. \quad (2)$$

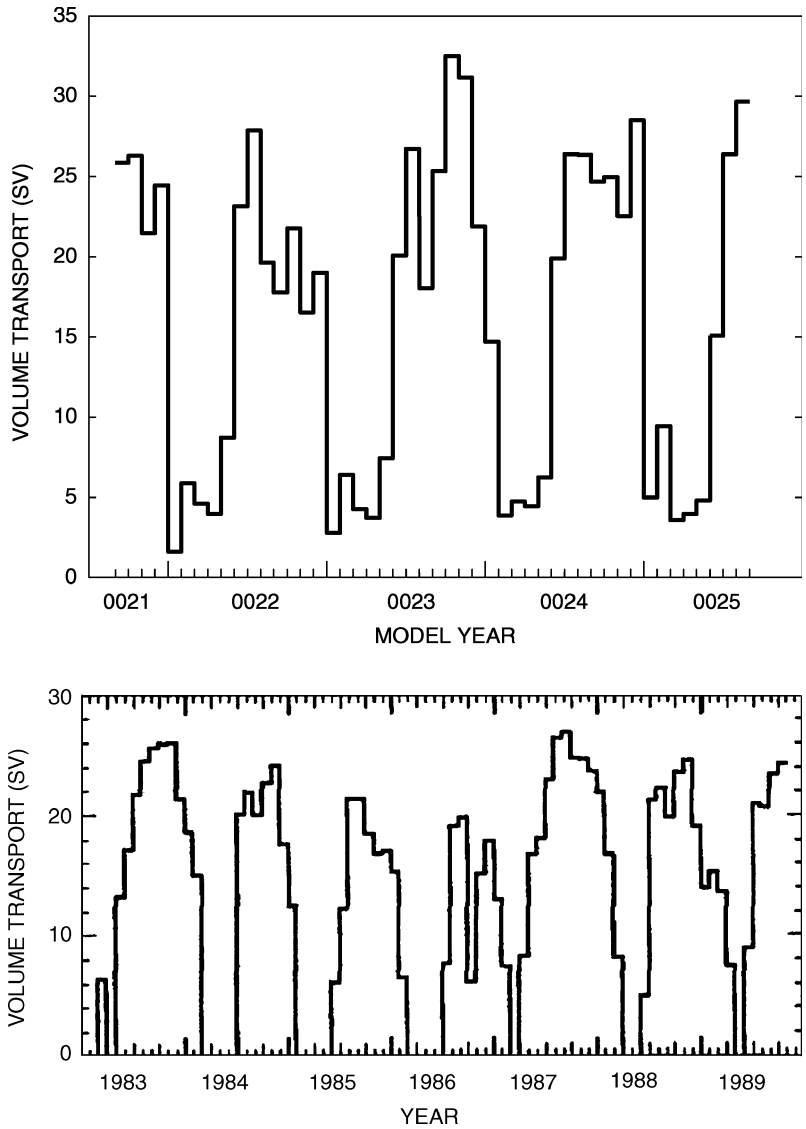

Fig. 2. Monthly averages of zonal geostrophic transport between 3°N and 9°N in the upper 500 m at 38°W (in Sv), for the model (top) and the observations (bottom, reproduced from Katz, 1993). Longer ticks on the *x*-axis mark the beginning of the calendar year.

However, at times the NECC is nonlinear and turbulent, and one might wonder whether it is reasonable to neglect the advection of relative vorticity in that region. A snapshot of the present model (Fig. 3) illustrates that, at a given time, it is not obvious how to establish the position of the mean current. The NECC appears as an accumulation of eddies. Here, we set out to understand and quantify the nonlinear contributions to the vorticity budget, which was not possible with the observations of Garzoli and Katz (1983).

3.2. Model results

The position of the core of the NECC shifts between 4.5°N (summer) and 8°N (winter; see Fig. 4a), as a result of the migration of the Inter-Tropical Convergence Zone (Garzoli and Richard-

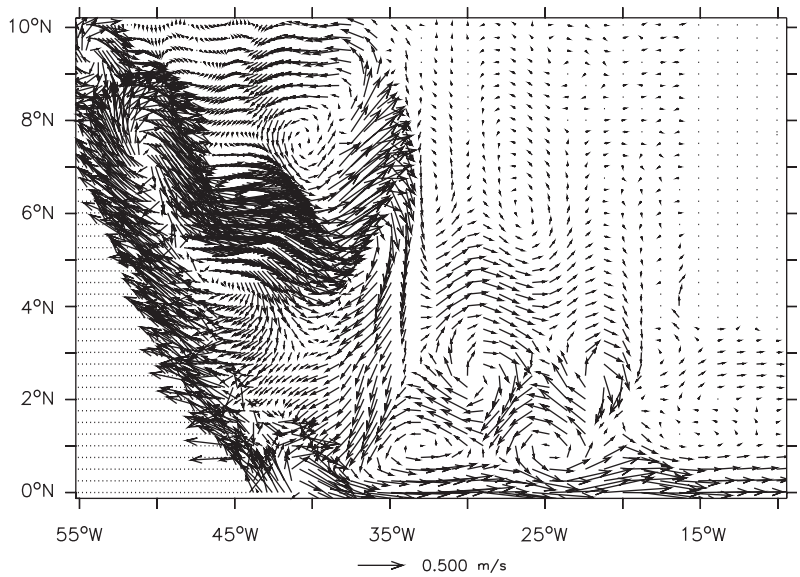

Fig. 3. Snapshot of the velocity in the tropical Atlantic at 100 m depth. The NECC appears as an accumulation of eddies.

son, 1989). To capture the NECC throughout the year, we analyze the vorticity equation between 4°N and 10°N. The frictional western boundary layer, west of 45–50°W, is excluded. Also, the eastern part of the current, flowing in the Gulf of Guinea, is not considered since the dynamics in that region are made more complex by the presence of the zonal boundary.

The wind stress curl is positive in most of the region of the NECC; thus Sverdrup's theory predicts northward transport in the interior of the gyre. This prediction is tested against the simulated fields by comparing the two terms of Eq. (2). Fig. 4b shows the model's meridional advection of planetary vorticity and the vortex stretching induced by the wind stress curl, zonally averaged between 45°W and 20°W. This region excludes the NBC. There is a good agreement with Sverdrup's theory north of 10°N, while in the region of the NECC (4–10°N), the advection of planetary vorticity does not balance the input of vorticity by the winds. In the region of the NECC the magnitude of the meridional flow appears to be larger than what can be accounted for by the wind stress curl. Between 5°N and 10°N, there is northward transport associated with the tropical gyre. South of 5°N, the meridional transport is negative due to a flow from the NECC to the EUC, in the western part of the basin below the Ekman layer. In those regions the nonlinearities neglected in the Sverdrup balance must be considered to close the vorticity budget.

Nonlinear advective terms account almost entirely for the departures from Sverdrup balance, as can be seen in Fig. 5, which shows the terms of Eq. (1) as a function of longitude. Friction is negligible everywhere except close to the western boundary. The vorticity equation is balanced within the total uncertainty of the mean values ($\frac{1}{N^2}\sqrt{\sum(x-\overline{x})^2}$ where N is the number of data points for the variable x).

In the western part of the basin, the dominant balance is between advection of planetary vorticity and advection of relative vorticity (by the mean flow and by the eddies). The contributions to the nonlinear advection are zonal advection of relative vorticity by the mean flow ($\overline{u}\frac{\partial}{\partial x}\overline{\zeta}$), meridional advection of relative vorticity by the mean flow ($\overline{v}\frac{\partial}{\partial y}\overline{\zeta}$), zonal advection of relative vorticity by the eddies ($\overline{u'\frac{\partial}{\partial x}\zeta'}$) and meridional advection of relative vorticity by the eddies ($\overline{v'\frac{\partial}{\partial y}\zeta'}$). The four components are examined separately in order to assess their relative importance and spatial distribution.

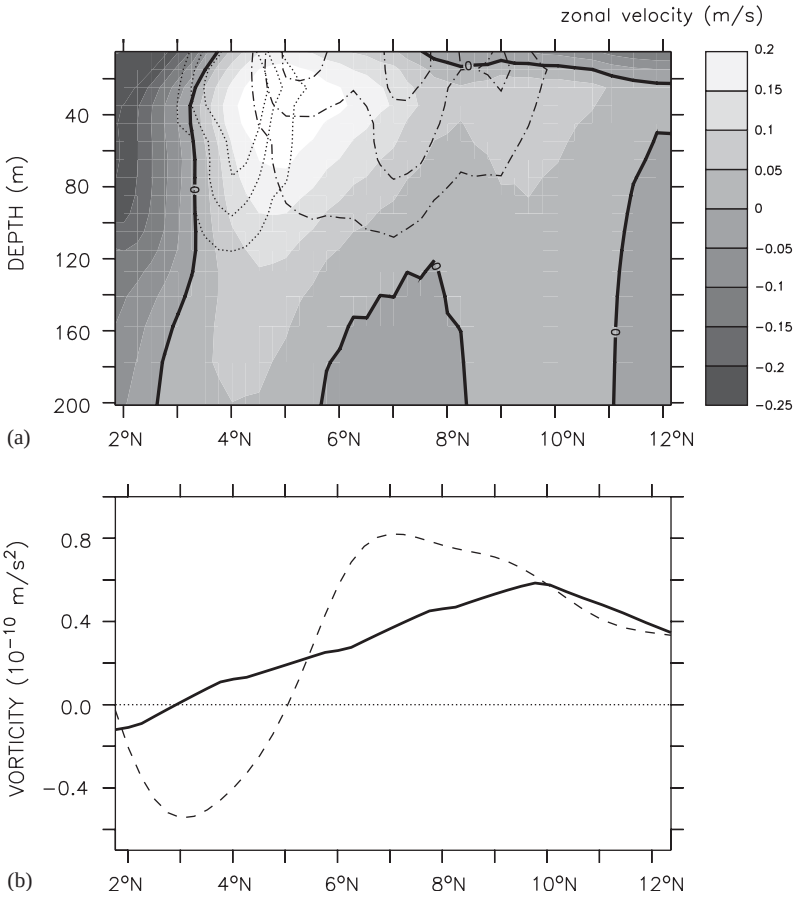

Fig. 4. (a) Annual mean zonal velocity at 30°W, illustrating the mean position of the core of the NECC. Contours show the southernmost and northernmost latitudes of the NECC core, occurring in the summer (dotted line) and winter (dash-dot line). (b) Both terms of the Sverdrup balance, averaged over the interior of the basin (45–20°W): input of vorticity by the winds (solid line) and meridional advection of planetary vorticity (dashed line).

Near the western boundary, the mean meridional flow is large and it is the northward advection of negative relative vorticity ($\frac{\partial \overline{v}}{\partial x} < 0$) by the mean flow which compensates for the northward advection of positive planetary vorticity. In the NBC/NECC retroflection, the zonal mean advection of relative vorticity is the important nonlinear term. Just east of the retroflection, the eddy field is strong and zonal eddy advection becomes important.

Fig. 6 shows the spatial distribution of the advection terms. They are plotted separately between 4°N and 7°N, and between 7°N and 10°N, in order to highlight the different regions of the western boundary current, the retroflection of the NBC, and the interior of the gyre. Those regions are aligned with the coastline rather than meridionally. We find that eddy advection of vorticity is opposed to the mean advection in the western boundary current as well as where the NBC retroflects, but that these two types of advection are the same direction in the interior of the gyre. Between 44°W and 32°W, zonal mean advection is the main nonlinear term in the region 4–7°N, whereas meridional mean advection and meridional eddy advection dominate in the region 7–10°N. East of 32°W, nonlinear terms are negligible and the flow is in Sverdrup balance.

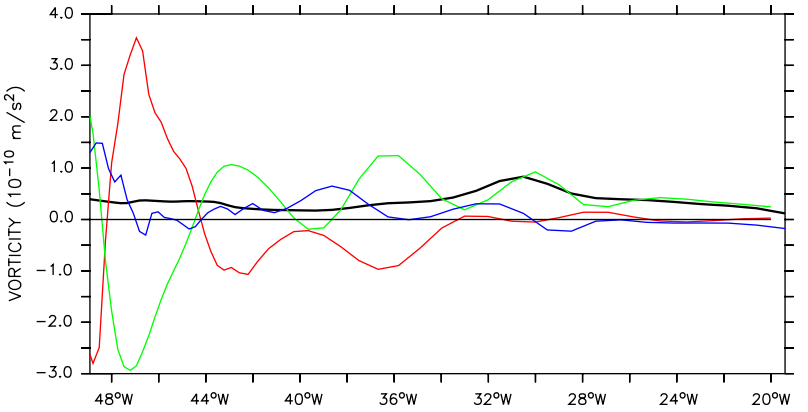

Fig. 5. Input of vorticity by the winds (black line) and meridional advection of planetary vorticity (green line), and nonlinear advection terms (red line) averaged between 4°N and 10°N. The blue line indicates the residual, which is mainly due to the uncertainty of the mean fields. The frictional term is significant only very near the western boundary and is not shown on this plot.

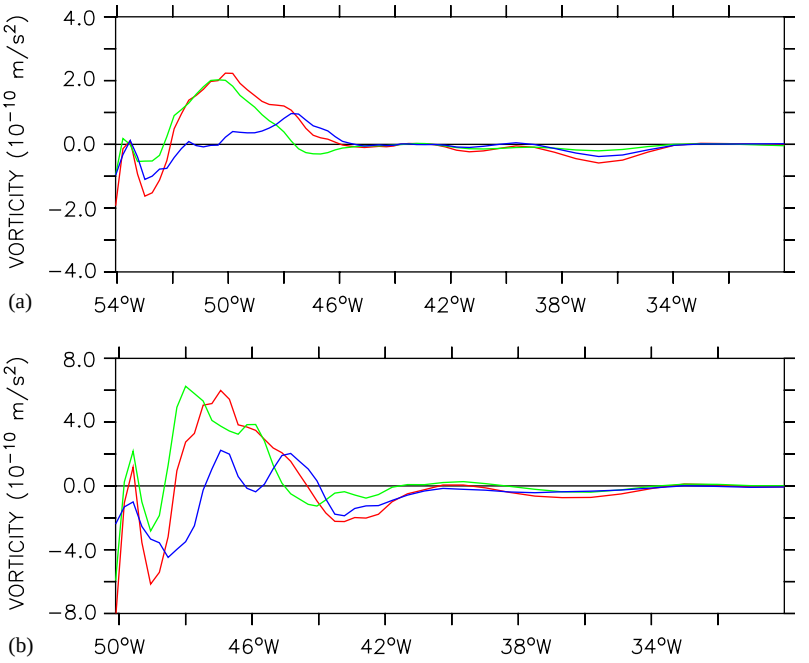

Fig. 6. Nonlinear advection terms (a) averaged between 7°N and 10°N; (b) averaged between 4°N and 7°N. Red line: total advection; green line: advection of mean relative vorticity by the mean flow; blue line: advection of eddy relative vorticity by the eddies (in 10^{-10} m/s^2). The eastern part of the basin, where nonlinearities are negligible, is not shown.

3.3. Comparison with observations

Our results differ from those of Garzoli and Katz (1983), who concluded based on observations that the NECC, between 3°N and 9°N, was in Sverdrup balance in the interior of the basin (from 42°W to 22°W). The difference lies in the extent of the region in which Sverdrup balance does not

hold: west of 42°W in Garzoli and Katz (1983), but west of 32°W in the present model. There are several possible reasons for this difference. The first and obvious one is that the model is not a perfect representation of the ocean. Mainly because of the idealized coastlines, but maybe also because of the variable grid spacing in the zonal direction, there is some uncertainty on the location where Sverdrup balance breaks down.

Other possible causes of discrepancy lie in the resolution and availability of observational datasets. Firstly, using historical hydrographic data leads to smoothing of spatial gradients, due to the coarse resolution of the data. Advective nonlinear terms will therefore be underestimated. Secondly, since velocity fields were not available from the observational study, the vorticity equation had to be written in terms of the seasonal thermocline depth, for a $1\frac{1}{2}$ layer ocean. The implicit assumption is that the ocean is at rest below the thermocline. In the observations as well as in our model, the seasonal thermocline has a mean depth of approximately 100 m. In our model the transports below 100 m, although smaller than the surface values, are not negligible; in the western part of the basin, the deep meridional transports can contribute up to 50% to the total meridional transport. Thus, due to observational constraints Garzoli and Katz (1983) could not account for two contributions to the vorticity equation: the nonlinear advection of relative vorticity, and the deep meridional advection of planetary vorticity. In our model, the deep meridional advection and the nonlinearities have opposite signs below the thermocline (Fig. 7). The partial cancellation of these two contributions could explain why Garzoli and Katz (1983), but not the present authors, found the flow between 42°W and 32°W to be in Sverdrup balance.

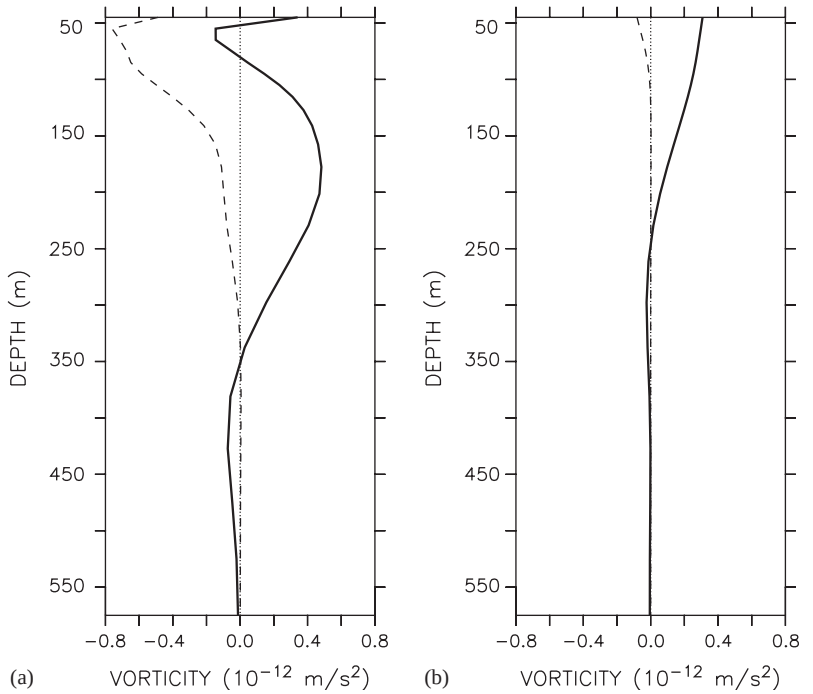

Fig. 7. Meridional advection of planetary vorticity (solid line) and nonlinear advection (dashed line) in the geostrophic interior (below the Ekman layer). Left panel is at 35°W/7°N, where Sverdrup balance does not hold; right panel at 25°W/7°N, where the Sverdrup balance is satisfied. The thermocline is about 100 m deep. In both cases the nonlinear terms and the transport below the thermocline have opposite signs, although their magnitude is less where the Sverdrup balance appears to be valid.

4. Discussion

A high resolution model of the tropical Atlantic is used to investigate the vorticity balance of the Atlantic NECC. The present study focuses on the nonlinear dynamics, which were not resolved in the observational study of Garzoli and Katz (1983). In the numerical model used here, it is found that nonlinear advection of relative vorticity, by the mean flow and by the eddies, is needed to close the vorticity budget in the western part of the basin. Since the model flow fields are similar to the observations, this result suggests that the Sverdrup balance is not valid in the western part of the real NECC either. The model, of course, cannot predict exactly where the Sverdrup balance breaks down, but our results strongly suggest that it is invalid in a larger area than previously thought. To determine the exact location it will be essential to get more observations, especially between 44°W and 32°W. An analysis of the vorticity balance using more recent datasets will give valuable information regarding the extent of the area within which the Sverdrup balance holds.

There are several other factors that could contribute to departures from the Sverdrup balance which have not been addressed here. One of them is the interannual variability of the winds; by relying on climatological forcing we filter out extreme years during which the Sverdrup balance might not hold. Another factor is the spatial resolution of the wind observations, which leads to a smoothing out of strong gradients. For the Pacific, Kessler et al. (2003) found that the use of wind fields based on QuickScat has a profound impact on the vorticity balance since it better resolves the sharp gradients in the wind field. Therefore the validity of the Sverdrup balance in the eastern basin could still be challenged.

In conclusion, our results suggest that the nonlinear dynamics may dominate the flow not only near the western boundary, but also in large parts of the interior of the tropical Atlantic. This has implications for our general understanding of the tropical ocean circulation. It is commonly assumed that the tropical oceans are governed by linear dynamics, partly because the early successes in El Niño forecasting with linear ocean models (Cane et al., 1986) supported this assumption. The present results suggest that, at least in the tropical Atlantic, nonlinear dynamics may need to be accounted for to understand the ocean circulation. Another interesting result is that the eddy advection of relative vorticity is a significant contributor to the vorticity balance almost everywhere west of 32°W. This not only makes it difficult to develop a theoretical framework for the NECC, but is also a challenge to any observational study.

The present results have implications for the study of climate as well. The NECC distributes the warmest water of the Atlantic ocean, which in turn determines the strength and location of tropical precipitation (Lindzen and Nigam, 1987). Therefore, an understanding of the heat transport by the NECC is necessary to predict interannual climate changes in the tropical Atlantic. Foltz et al. (2003) showed with PIRATA mooring data that meridional advection of heat is a significant part of the heat budget at 8°N/38°W; here it is shown that this meridional advection may depend not on local wind, but rather on the difficult to determine nonlinear processes.

Acknowledgements

The authors acknowledge the support of Paola Malanotte-Rizzoli and John Marshall. They are grateful to Silvia Garzoli and one anonymous reviewer for comments that helped to improve the manuscript. This research was funded by NASA Grant NAG5-7194 and NOAA Grant NA16GP1576 at MIT. The computations were performed at the NCAR facilities in Colorado and the results were analyzed with Ferret software.

References

Cane, M.A., Dolan, S.C., Zebiak, S.E., 1986. Experimental forecasts of the 1982/83 El Niño. Nature 321, 827–832.

Enfield, D.B., Mayer, D.A., 1997. Tropical Atlantic SST variability and its relation to ENSO. Journal of Geophysical Research 102, 929–945.

Foltz, G.R., Grodsky, S.A., Carton, J.A., McPhaden, M.J., 2003. Seasonal mixed layer heat budget of the tropical Atlantic ocean. Journal of Geophysical Research 108, 3146, doi: 10.1029/2002 JC 001584.

Fratantoni, D.M., Johns, W.E., Townsend, T.L., Hurlburt, H.E., 2000. Low-latitude circulation and mass transport in a model of the tropical Atlantic ocean. Journal of Physical Oceanography 30, 1944–1966.

Garzoli, S.L., Katz, E.J., 1983. The forced annual reversal of the Atlantic North Equatorial Countercurrent. Journal of Physical Oceanography 13, 2082–2090.

Garzoli, S., Richardson, P.L., 1989. Low-frequency meandering of the Atlantic North Equatorial Countercurrent. Journal of Geophysical Research 94, 2079–2090.

Hellerman, S., Rosenstein, M., 1983. Normal monthly wind stress over the world ocean with error estimates. Journal of Physical Oceanography 13, 1093–1104.

Jochum, M., Malanotte-Rizzoli, P., 2001. On the influence of the meridional overturning circulation on the tropical–subtropical pathways. Journal of Physical Oceanography 31, 1313–1323.

Jochum, M., Malanotte-Rizzoli, P., 2003. On the generation of North Brazil Current rings. Journal of Marine Research 61, 147–173.

Jochum, M., Malanotte-Rizzoli, P., Busalacchi, A., 2004. Tropical instability waves in the Atlantic Ocean. Ocean Modelling 7, 145–163.

Katz, E.J., 1993. An interannual study of the Atlantic North Equatorial Countercurrent. Journal of Physical Oceanography 23, 116–123.

Kessler, W.S., Johnson, G.C., Moore, D.W., 2003. Sverdrup and nonlinear dynamics of the pacific equatorial currents. Journal of Physical Oceanography 33, 994–1008.

Leetmaa, A., McCreary Jr., J.P., Moore, D.W., 1981. Equatorial currents: observations and theory. In: Warren, B.A., Wunsch, C. (Eds.), Evolution of Physical Oceanography. MIT Press, Cambridge, pp. 184–196.

Lindzen, R., Nigam, S., 1987. On the role of SST gradients in forcing low level winds and convergence in the tropics. Journal of the Atmospheric Sciences 44, 2418–2436.

Liu, Z., Philander, S.G.H., 1995. How different wind stress patterns affect the tropical-subtropical circulations of the upper ocean. Journal of Physical Oceanography 25, 449–462.

Murtugudde, R., Seager, R., Busalacchi, A., 1996. Simulation of the tropical oceans with an ocean GCM coupled to an atmospheric mixed layer model. Journal of Climate 9, 1796–1815.

Pedlosky, J., 1979. Geophysical Fluid Dynamics. Springer, New York.

Philander, S.G., 1990. El Niño, La Niña and the Southern Oscillation. Academic Press, London.

Richardson, P.L., Arnault, S., Garzoli, S., Bruce, J.G., 1992. Annual cycle of the Atlantic North Equatorial Countercurrent. Deep Sea Research 39, 997–1014.

Sverdrup, H.U., 1947. Winddriven currents in a baroclinic ocean with application to the equatorial currents in the eastern Pacific. Proceedings of the National Academy of Sciences USA 33, 318–326.

Wunsch, C., Roemmich, D., 1985. Is the North Atlantic in Sverdrup balance. Journal of Physical Oceanography 15, 1876–1880.

Yu, Z., McCreary, J.P., Kessler, W., Kelly, K.A., 2000. Influence of Equatorial dynamics on the Pacific North Equatorial Countercurrent. Journal of Physical Oceanography 30, 3179–3190.